Carbohydrate Polymers 98 (2013) 951–958

Contents lists available at SciVerse ScienceDirect

Carbohydrate Polymers

journal homepage: www.elsevier.com/locate/carbpol

Formation and characterization of chitosan-polylacticacid-polyethylene glycol-gelatin nanoparticles: A novel biosystem for controlled drug delivery

M. Rajan [1], V. Raj *

Advanced Materials Research Laboratory, Department of Chemistry, Periyar University, Salem- 636 011, Tamilnadu, India

ARTICLE INFO

Article history:
Received 14 December 2012
Received in revised form 11 May 2013
Accepted 14 May 2013
Available online 21 May 2013

Keywords:
Chitosan
Drug delivery
Encapsulation
Gelatin
Nanoparticles
Polyethylene glycol
Rifampicin

ABSTRACT

Chitosan (CS)–polylacticacid (PLA)–polyethylene glycol (PEG)–gelatin (G) nanoparticles, a novel drug vehicle for the controlled release of an antitubercluosis drug, rifampicin (RIF) was developed and its chemical and biochemical activities were studied by various standard methods. The designed carriers CS, PEG and G nanoparticles were prepared by emulsion solvent evaporation technique, and then used for entrapping RIF. Linking was confirmed by FTIR spectroscopy. The surface morphology of the nanoparticles was studied using scanning electron microscope and polarizing microscope. The influence of process variables, on particle size, zeta potential and matrix entrapment of RIF was studied. The encapsulation and loading capacity were evaluated, and an in vitro release of RIF was assessed using the dialysis method. The effect of nanoencapsulation of RIF on the antibacterial activity of RIF against Mycobacterium strains was evaluated. The preliminary results clearly suggested that the cross linked CS–PLA–PEG–G matrix may be a potential polymeric carrier for controlled delivery of RIF.

1. Introduction

Tuberculosis (TB), the second most deadly contagious and airborne infectious disease, is a chronic granulomatous bacterial infection. Tuberculosis still remain an infectious disease especially in India. The global scourge of multi-drug resistant TB is attaining epidemic proportions and is most prevalent in developing countries, with elevated rates of human immunodeficiency virus infection (HIV) (Du Toit, Pillay, & Danckwerts, 2006). Current treatment for TB consists of frequent high dosing of combinations of oral anti-tuberculosis drugs. It is usually treated by taking one medicine for 9 months. The yearlong chemotherapy in pulmonary tuberculosis results in dose related side effects and may not reach atelectatic areas. This method of treatment, however, causes systemic toxicity and undesired side effects while the intensive regimen leads to patient non-compliance (Schreiber, Zissel, Greinert, Schlaak, & Muller-Quernheim, 1999). Whereas, in active TB, the bacteria are active in the body and immune system is unable to stop them from causing tissue damage. Since the bacilli are able to survive in the host body for years, about 92% of the new cases of clinical tuberculosis arise in individuals who have been infected by tuberculosis previously (Klaudt, 2000). According to World Health Organization (WHO), approximately one-third of the global population is infected with *Mycobacterium tuberculosis* and more than nine million people develop active TB every year, and approximately two million die annually (The Union, 2013). To avoid systemic toxicity and maximize drug effectiveness, anti-tuberculosis drugs are also being formulated for direct delivery to the affected site and prolong effect in the deep regions of the lungs.

Characterization of a drug molecule becomes extremely important when it is related with one of the detrimental diseases and very few of such drugs are available for the management of such diseases. Tuberculosis (TB) is an example of such disease for which limited number of antibiotics, for example, rifampicin, isoniazid, and ethambutol, are the essential choices for the clinical disease management (Rajan & Raj, 2012). Among others, rifampicin (RIF) is a first-line drug for use in the therapy of tuberculosis and is included in the list of recommended drug regimens for treatment of latent M. tuberculosis infection in adults (Centers for Disease Control, 2000). A number of drug delivery systems were developed for the release of RIF, isoniazid for use in therapy of tuberculosis (Booysen et al., 2013; Chan et al., 2013; He et al., 2013; Mehta & Neha, 2013; Singh,

* Corresponding author. Tel.: +91 9790694972.
E-mail addresses: rajanm153@gmail.com (M. Rajan), alaguraj2@rediffmail.com (V. Raj).
[1] Tel.: +91 9488014084.

0144-8617/$ – see front matter © 2013 Published by Elsevier Ltd.
http://dx.doi.org/10.1016/j.carbpol.2013.05.025

Bhandari, & Indu Pal, 2013; Wu et al., 2013). Despite being an effective drug molecule, treatment of TB with RIF still faces a number of challenges. Firstly, the oral delivery of RIF can cause a number of serious side effects including hepatotoxicity (Changsan, Chan, Separovic, & Srichana, 2009). Secondly, RIF exhibits concentration-dependent activity, meaning that its therapeutic activity is directly proportional to its concentration at the target site (Gumbo et al., 2007). Although, RIF is poorly soluble in aqueous media, it is a clinically effective drug. The inescapable necessity and poor solubility of RIF automatically necessitates an alternate drug delivery/carrier system (Hillmyer, 2007; Huwyler, Wu, & Pardridge, 1996; Langer, 2001; Mehta, Bhasin, Mehta, & Dham, 2005; Sullivan & Huang, 1986). In this regard, the interaction of RIF with various potential drug carrier systems is essential. However, such studies on the encapsulation of the drug in other macromolecules/molecular assemblies in present literature are sparse.

Recently, much attention has been paid to utilizing chitosan (CS) and its derivatives for drug delivery vehicles, wound healing accelerators, and nerve regeneration agents (Geng, Yonglong, Qing, Mozhen, & Yuee, 2008). CS nanoparticles could elicit dose-dependent inhibitory effects on the proliferation of various tumor cell lines, while low toxicity against normal human liver cells. However, the application of CS suffers severe limitations because of its poor solubility both in water and organic solvents due to its rigid crystalline structure. To overcome this deficiency, a variety of graft copolymers of chitosan were synthesized and used for drug delivery systems (Jayakumar, Reis, & Mano, 2006; Kweon & Kang, 1999). The most widely used classes of biocompatible and biodegradable polymers, approved by Food and Drug Administration (FDA), is that of aliphatic polyester, including poly (lactic acid) (PLA), poly (glycolic acid) (PLGA) and their copolymers. Due to its good mechanical properties, like biocompatibility, biodegradation, excellent thermal/mechanical properties and superior transparency of these materials (Tzong-Ming & Cheng-Yang, 2006; Yan et al., 2009) they have been widely used in surgical sutures, drug delivery systems and tissue engineering (Rahul, Amol, & Douglas, 2010).

The present work is devoted to the preparation of novel self-assembled nanoparticles by conjugating different bioactive compounds. CS–PLA is blended with polyethylene glycol (PEG) and gelatin (G) by emulsion solvent evaporation technique. The emulsion solvent evaporation method is the widely used one among various encapsulation techniques. Various drugs are successfully retained within particles prepared by this method. Many types of pharmaceuticals and biopharmaceuticals with different physico-chemical properties have been formulated into particles by emulsion method. The emulsion method has been considered better since the method is relatively simple, convenient in controlling process parameters, and has the ability to produce with simple instrument. The advantages of the bioactivity of CS–PLA–PEG–G matrix along with the attractive properties of matrix have been presented. The developed composite nanoparticles have been characterized and evaluated for in vitro studies, cell inhibition studies and instrumental characteristics. The developed composite nanoparticle is a soft matrix material and can be utilized for tuberculosis treatment and drug delivery. The results obtained have been discussed in detail in this paper.

2. Materials and methods

2.1. Materials

CS derived from crab shell, was purchased from Otta Chemika–Biochemika reagents, India. PLA, dichloromethane, PEG, gelatin, poly (ethylene oxide) (PEO), phosphate buffer saline (PBS) and acetic acid were obtained from Merck Chemical Company Inc. (Mumbai, India). Rifampicin drug was purchased from Sigma Chemicals, India. All other chemicals were of analytical grade and used as such without further purification.

2.2. Preparation of CS–PLA nanoparticles

The CS–PLA nanoparticles were prepared by following the reported method (Ashish Dev et al., 2010) with a slight modification. About 120 mg of PLA was dissolved in 10 ml of dichloromethane to form a fine dispersion. This solution was rapidly poured into 10 ml of 1% acetic acid solution containing 60 mg of CS and 200 mg of PEO. The mixture was sonicated for 60 min to form an emulsion and vigorously stirred until the organic solvent is evaporated. By addition of water the nanoparticles were precipitated and then cooled at 10 °C. Finally, the nanoparticles suspension was evaporated using rotary evaporator.

2.3. Preparation of rifampicin loaded CS–PLA nanoparticles

To encapsulate hydrophobic drug, w/o/w emulsion technique was applied. Aqueous drug solution was first poured into a polymer solution (120 mg of PLA dissolved in 10 ml dichloromethane) to form a w/o emulsion. The w/o emulsion was then rapidly poured into 10 ml of 1% acetic acid solution containing 60 mg of CS and 200 mg of PEO. The mixture was sonicated for 60 min to form an emulsion, and then vigorously stirred. Stirring was continued until the organic solvent is evaporated. By the addition of water, the nanoparticles were precipitated and then cooled at 10 °C. Finally, the nanoparticles evaporated using rotary evaporator. Then the above mentioned procedure was followed and added PEG and gelatin to an appropriate portion of 1% acetic acid solution containing 60 mg of CS and 200 mg of PEO, followed by continuous stirring until the organic solvent is evaporated. By the addition of water the nanoparticles were precipitated and then cooled at 10 °C. Finally, the nanoparticles were evaporated using rotary evaporator. The prepared nanoparticles were named as chitosan–polylacticacid encapsulated rifampicin (CS–PLA–RIF), chitosan–polylacticacid–polyethylene glycol encapsulated rifampicin (CS–PLA–RIF–PEG) and chitosan–polylacticacid–polyethylene glycol–gelatin encapsulated rifampicin (CS–PLA–RIF–PEG–G).

2.4. Particle size

The particle size, size distribution and zeta potential of drug loaded nanoparticles were measured in a Zetasizer (Malvern instruments DTS Ver 4.10).

2.5. Morphological and FTIR analysis of nanoparticles

Scanning electron microscopy (SEM) and Polarizing microscope (Euromax, Holland) were used for the morphological analysis of the RIF, CS–PLA–RIF and PEG, G bind CS–PLA–RIF–PEG and CS–PLA–RIF–PEG–G nanoparticles. The FTIR spectra of samples were recorded using a Fourier transform infrared spectrometer (Spectrum GX-1, PerkinElmer, USA). Briefly, a small quantity of nanoparticles was mixed with 200 mg KBr and compressed to form pallets. These pallets were scanned, in transmission mode, in the spectral region of 4000–400 cm^{-1}, using a resolution of 4 cm^{-1} and 32 co-added scans.

2.6. Evaluation of drug loading capacity and encapsulation efficiency

The nanoparticles suspensions were separated with a centrifuge at 1250 rpm for 30 min, and the drug encapsulation efficiency (EE) and loading capacity (LC) of nanoparticles were evaluated by measuring the absorption of the supernatant using UV spectrophotometer (Systronics, India). The corresponding calibration curves were made by testing the supernatant of blank nanoparticles. Each sample was measured in triplicate. The absorption of RIF was measured at the λ_{max} value of 333 nm. The EE and LC of RIF of the CS–PLA, CS–PLA–PEG and CS–PLA–PEG–G nanoparticles were calculated according to the following equations (Papadimitriou, Bikiaris, Avgoustakis, Karavas, & Georgarakis, 2008):

$$EE = \frac{W_t - W_f}{W_t} \quad (1)$$

$$LC = \frac{W_t - W_f}{W_n} \quad (2)$$

W_t represents the total amount RIF; W_f is the amount of free RIF in the supernatant; and W_n is the weight of nanoparticles after freeze-drying. All measurements were performed in triplicate and the mean value was reported.

2.7. Evaluation of in vitro drug release

The evaluation of drug release was performed at 37 °C using the dissolution tester (Disso test, Lab India, Mumbai, India) equipped with six paddles at a paddle speed of 100 rpm. About 900 ml of phosphate buffer solution (pH 1.2 and 6.8) was used as the dissolution media to stimulate the gastrointestinal tract (GIT) conditions. A 5 ml aliquot was used each time for analyzing the rifampicin content at a fixed time interval. The dissolution media were replenished with a fresh stock solution. The amount of rifampicin released was analyzed using a UV spectrophotometer (Systronics, India) at the λ_{max} value of 333 nm.

2.8. Cell inhibition study

A modified broth microdilution method was employed (Coban, Birinci, Ekinci, & Durupinar, 2004) for preliminary screening, of *Mycobacterium* strains. *Mycobacterium smegmatis* bacterium was used in this study. The organism was subcultured into Middlebrook 7H9 broth in screw capped tubes and incubated at 37 °C for 7 days. Growth was observed and the tubes were then left at room temperature for the solid particles to sediment. The homogenous suspension at the upper part of the tube was then transferred into sterile screw capped tubes and measured at an optical density of 0.2–0.3 at 650 nm after which the cells were diluted 1000-fold in 7H9-medium. Susceptibility testing was performed in clear 96-well plates containing 50 μl of 7H9 liquid medium in each well except the first well. Drug or fractions, 10–100 μg/ml concentration, were used for the antimycobacterial assay. The drug was prepared at varying concentrations in 100% DMSO. The drug was vortexed and 100 μl of it dispensed into the first column (of the first row). 90 μl of extract solution with fresh medium was then transferred to give 2-fold serial dilutions. The diluted inoculation (10 μl) was dispensed into each of the wells, giving a final volume of 100 μl per well. This caused a further 2-fold dilution of the potential inhibitors in the wells. The plates covered in Ziploc bags, were incubated for 5–7 days at 37 °C. RIF was used as positive control while the cells were used as negative control. The assay was carried out in duplicate. MIC values were determined as the lowest concentration that inhibited the complete visible growth of the organism. The inhibition was assessed by alamar blue staining method.

Table 1
The particle size of CS–PLA–RIF, CS–PLA–RIF–PEG and CS–PLA–RIF–PEG–G.

% of RIF concentration	Particle size (nm) mean ± SD[a]		
	CS–PLA–RIF	CS–PLA–RIF–PEG	CS–PLA–RIF–PEG–G
10	187 ± 10.1	192 ± 08.5	197 ± 10.4
20	195 ± 12.4	202 ± 09.8	202 ± 11.6
30	201 ± 14.2	214 ± 12.1	214 ± 13.5
40	210 ± 15.9	222 ± 13.5	222 ± 14.6
50	214 ± 17.3	234 ± 15.2	234 ± 16.8

RIF, rifampcin; CS, chitosan; PEG, polyethylene glycol 600; PLA, poly lactic acid; TPP, sodium tripolyphosphate; SD, standard deviation for three determinations.
[a] $n = 3$. The experiments were repeated twice.

3. Results and discussion

3.1. Characterization of the prepared nanoparticles

3.1.1. Particle size and zeta potential of the prepared nanoparticles

Particle size is one of the important properties that influence in vivo performance. The smaller particle sizes will ensure lowered level of reticuloendothelial system (RES) uptake, improve utilization ratio of drug and diminish drug side effects. Table 1 and Fig. 1 depict particle size and zeta potential of CS, PEG and G coated with different RIF concentrations. In the case of CS–PLA–RIF, particle size of which was 187 nm, possessed the zeta potential of 21 ± 2.2 mV. With the increasing amount of RIF coating from 10% to 50%, particle size and zeta potential values increased from 187 to 214 and 21 ± 2.2 to 29 ± 1.6 mV respectively, owing to the interaction between the RIF and the CS–PLA surface. Meanwhile, particle size rises slightly along with the augment of PEG and G additions, representing 192 and 197 with the concentration of 10% RIF, respectively. As the RIF amount was up to 50%, a significant difference was implied in respect of particle size, however, the zeta potential came to a relatively constant value. It can be concluded, that the coating layer had reached a saturated status in the presence of 50% RIF, and excessive amount of RIF in the solution would not change the coating strength and zeta potential of CS–PLA, CS–PLA–PEG and CS–PLA–PEG–G, instead, they lead to a sharp rise with regard to particle size. And also the value of zeta potential less than −30 mV or higher than +30 mV can be used to assure the stability of nanoparticles suspensions. The values obtained for the prepared nanoparticles were above +30, so it was stable. The positive values obtained for zeta potential indicates that the nanoparticles surface was positively charged. This may be due to the availability of chitosan free NH_3^+ groups on the polymer surface (Rajan & Raj, 2012).

3.1.2. Surface morphology

SEM images confirmed the formation of particles with a log-normal particle sized distribution. The SEM showed that all the

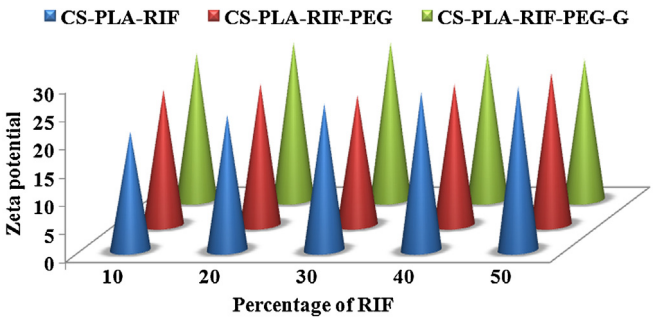

Fig. 1. The zeta pontential values of CS–PLA–RIF, CS–PLA–RIF–PEG, CS–PLA–RIF–PEG–G with various concentrations.

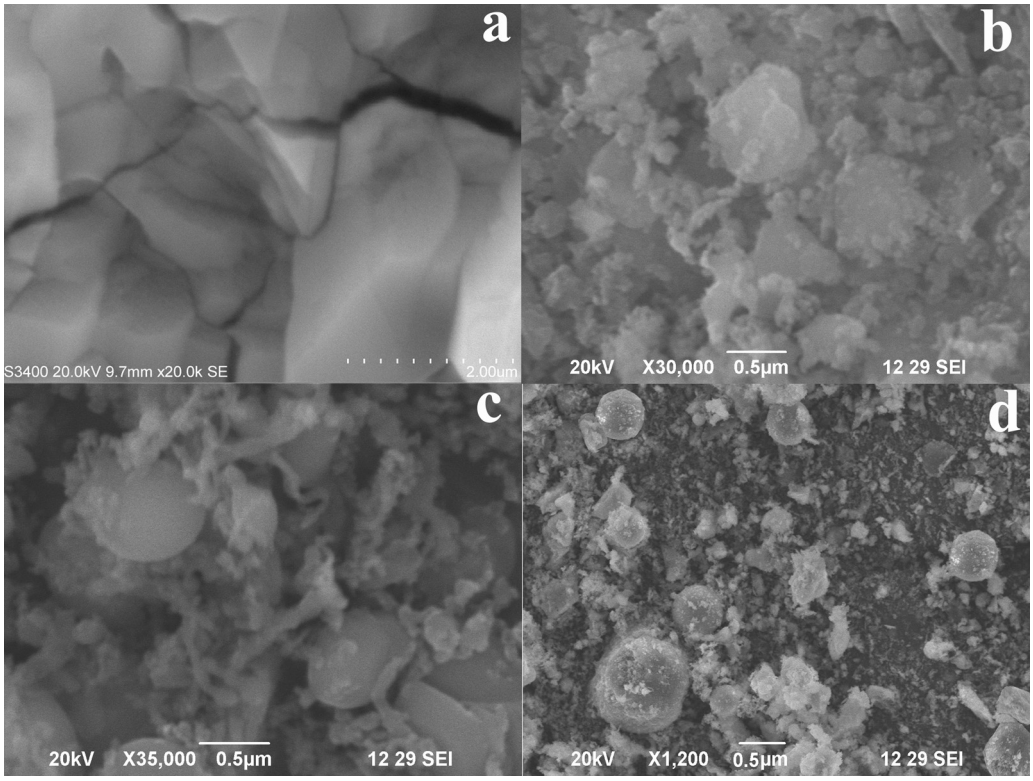

Fig. 2. SEM images of rifampicin (a), CS–PLA–RIF (b), CS–PLA–RIF–PEG (c) and CS–PLA–RIF–PEG–G (d).

CS–PLA–RIF, CS–PLA–RIF–PEG and CS–PLA–RIF–PEG–G nanoparticles were spherical and compact (Fig. 2). The morphology of the polyelectrolyte complex (Figs. 1c, d and 2b) appears homogenous, indicating a uniform distribution and a good compatibility between RIF and coated polymers. CS–PLA–RIF showed the smaller particle and fine, flake-like particles compared to other two nanoparticles. CS–PLA–RIF–PEG showed the highest tapped densities due to their compact morphology, whereas CS–PLA–RIF–PEG–G showed the good spherical due to its higher granulometry and porosity (Fig. 2). This observation is consistent with the general morphology of nanoparticles formed using combinations of emulsion solvent evaporation methodologies, where, such particles often being described as spherical like structures. The polarizing microscopy studies (Fig. 3) show that CS–PLA–RIF, CS–PLA–RIF–PEG and CS–PLA–RIF–PEG–G nanoparticles are spherical in shape. The freshly prepared particles clearly show the spherical microstructure of the CS–PLA–RIF, CS–PLA–RIF–PEG and CS–PLA–RIF–PEG–G nanoparticles. CS–PLA–RIF, CS–PLA–RIF–PEG and CS–PLA–RIF–PEG–G nanoparticles are uniform in shape with a vesicular structure and porous nature. The optical images show the increseing of particle population and morphological features from CS–PLA–RIF, CS–PLA–RIF–PEG and CS–PLA–RIF–PEG–G composites. It depicts that the optical images of the RIF encapsulated nanoparticles sizes are correlated with the SEM images. And also the size of the drug encapsulated nanoparticles has also been confirmed using zeta analyzer. Different from nanoparticles showed an irregular and amorphous shape, suggesting that the formation of a molecular inclusion complex of RIF.

3.1.3. *Fourier transmission infra red spectroscopy (FTIR)*

In order to confirm the CS–PLA–PEG–G interaction to RIF, samples were analyzed by FT-IR spectroscopy shown in Fig. 4. Fig. 4a shows the FTIR spectra of CS–PLA, CS–PLA–PEG and CS–PLA–PEG–G complexes formed at 10% of RIF. CS is an amino glucose characterized by a small proportion of amide groups via an amide linkage with acetic acid. The FTIR of CS–PLA–RIF, CS–PLA–RIF–PEG and CS–PLA–RIF–PEG–G showed peaks around 946 cm^{-1} and 1068 cm^{-1} of assigned saccharine structure, and a strong amide

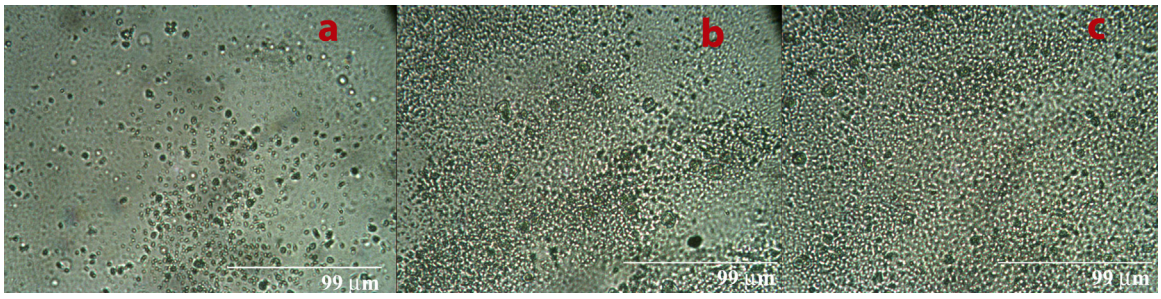

Fig. 3. Optical images of CS–PLA–RIF (a), CS–PLA–RIF–PEG (b) and CS–PLA–RIF–PEG–G (c).

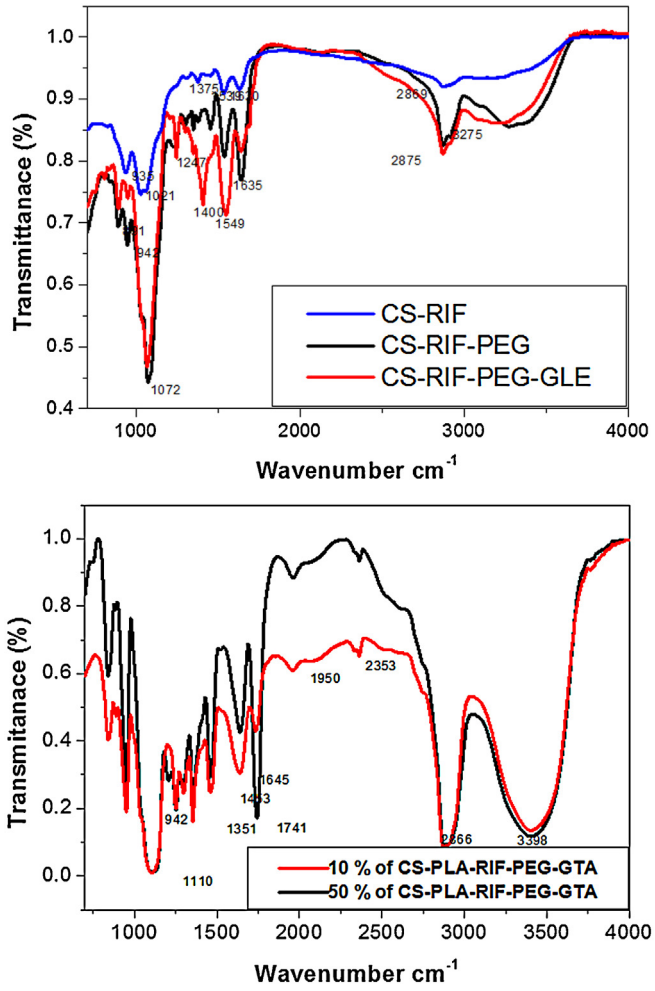

Fig. 4. FTIR spectra of CS–PLA–RIF, CS–PLA–RIF–PEG and CS–PLA–RIF–PEG–G (a), and 10–50% of RIF encapsulated CS–PLA–RIF–PEG–G (b).

characteristic peak at 1635 cm^{-1} as well as a characteristic peak assigned to protonated amine, at around 1539 cm^{-1}. The shift in amine band to 1539 cm^{-1} in the spectrum of complexes indicates a change in environment of amine group through its interaction with gelatin. Fig. 4b shows the FTIR spectra of CS–PLA–PEG–G complexes formed at 10% and 50% of RIF. The spectra of the different concentration of RIF coated polymer matrix was varied only the intensity of the peaks. In fact the complexes were stabilized by electrostatic interaction between positively charged chitosan (NH_3^+) and negatively charged pectin (COO^-). Moreover there also exists the possibility of intramolecular H-bonding between the COOH groups of pectin or NH_2 groups of chitosan and OH, OCH_3 or $COOCH_3$ groups elsewhere within the complex. Moreover, an increasing intensity of $-NH_3^+$ group band can be observed in the spectra of CS–PLA–PEG–G complex (Rashidova et al., 2004). However, the peak sizes were smaller that could be due to the smaller amount of addition of polymer entrapped in the polymer matrix.

3.2. Encapsulation efficiency and loading capacity of nanoparticles

The initial concentration of RIF plays an important role in the EE and LC of CS–PLA, CS–PLA–PEG and CS–PLA–PEG–G nanoparticles (Table 2). When the concentration of RIF is increased, the EE of CS–PLA, CS–PLA–PEG and CS–PLA–PEG–G polymer combination is increased. The EE of CS–PLA–PEG–G nanoparticle is slightly greater than that of the CS–PLA and CS–PLA–PEG nanoparticles. The high %EE for 50% of RIF has been found to be 67.2%, 82.6%, and 96.8% of the CS–PLA, CS–PLA–PEG and CS–PLA–PEG–G composites, respectively than the reported composites (Desai & Park, 2005; Jelvehgari, Nokhodchi, Rezapour, & Valizadeh, 2010). However, the increase in RIF concentration leads to an increase of both EE and LC of polymer nanoparticles. It was found that the EE and LC of CS–PLA–PEG–G nanoparticles are higher than that of CS–PLA and CS–PLA–PEG combination nanoparticle when the initial concentration of RIF is same, which could be attributed to the fact that CS–PLA–PEG–G nanoparticles has a more electrostatic attraction than CS–PLA and CS–PLA–PEG combination nanoparticles with RIF.

3.3. In vitro release studies

Various techniques have been described for the study of drug release from nanocarrier systems. The dialysis method has been frequently reported for this purpose as it facilitates the separation of the released drug from the bound drug. However, the release rate of the drug is usually affected by the diffusional resistance of the membrane. Fig. 5 shows the results of continuous dissolution of RIF from the CS–PLA, CS–PLA–PEG and CS–PLA–PEG–G coated controlled delivery system in artificial gastric fluid (pH 1.2) and artificial small intestinal fluid (pH 6.8). The percentage release of RIF from CS–PLA was somewhat greater when compared to that of CS–PLA–PEG and CS–PLA–PEG–G combined nanoparticles. The CS–PLA–RIF, CS–PLA–RIF–PEG and CS–PLA–RIF–PEG–G coated nanoparticles, the percentage of RIF released from the nanoparticles initially rapid and then very slow after some hours, which was consistent with the phenomena reported by other authors (Chen et al., 2009, 2011; Yang et al., 2008; Zhang et al., 2009). The release profiles at the both pH, one can easily see that, for the same drug loading, the release rate of RIF increases when the pH of the release medium increases (Fig. 5). It would appear, that the rate of RIF release from the CS–PLA, CS–PLA–PEG and CS–PLA–PEG–G coated nanoparticles depends on the dissolution capacity of the particles at the particular release medium used. These results indicated that the prepared nanoparticles are useful controlled delivery system for TB treatment. The electrostatic attraction between drug and CS–PLA–PEG–G polymer composite is higher than the drug and CS–PLA and CS–PLA–PEG polymer composite. This suggests that the drugs in the composites can be easily released into the basic than acidic environment. Because, the electrostatic interaction of composites is more easily broken at pH 6.8 than at pH 1.2, leading to rifampicin being released more rapidly at pH 6.8 than pH 1.2. The prepared nanocarrier composites are good releasing rate in both pH medium than other reported systems (Singh et al., 2013).

3.4. Cell inhibition studies

The interaction of free RIF and RIF loaded CS–PLA, CS–PLA–PEG and CS–PLA–PEG–GLE nanoparticles with *M. smegmatis* was investigated to understand the applicability of such particles. The growth of the relative cells vability in the presence of free drug added at time zero is also shown in Table 3 and Fig. 6. Growth studies were done in the presence of free drug ie, RIF and RIF loaded CS–PLA, CS–PLA–PEG and CS–PLA–PEG–GLE nanoparticles. Significant change in growth behavior was observed. The total yield of cells was high in the stationary phase when compared to the control. The growth of *M. smegmatis* cells in the presence of CS–PLA, CS–PLA–PEG and CS–PLA–PEG–G with 50% of RIF drug confirmed that the composites or the polyelectrolytes used to make these composites are not toxic to the microbial cells and does not affect either the growth rate or the yield in a significant way indicating that the composites are cytocompatible. As compared to the other two nanocomposites CS–PLA–RIF–PEG–G was not toxic and

Table 2
Encapsulation efficiency (EE) and loading capacity (LC) of CS nanoparticles.

S. no.	% of RIF	CS–PLA–RIF nanoparticle		CS–PLA–RIF–PEG nanoparticle		CS–PLA–RIF–PEG–G nanoparticle	
		% of EE	% of LC	% of EE	% of LC	% of EE	% of LC
1	10	47.4	12.5	61.6	16.3	72.4	20.8
2	20	52.1	20.2	68.1	25.4	78.8	31.2
3	30	57.9	30.9	74.9	39.1	89.2	38.7
4	40	64.5	41.1	78.4	52.4	92.4	48.4
5	50	67.2	50.2	82.6	74.8	96.8	69.7

good inhibition effects. An important point to note is that the encapsulated capsules released 50% RIF from CS–PLA, CS–PLA–PEG and CS–PLA–PEG–G composites acts with the same efficacy as the free drug. Thus, indirectly it can be concluded that, the drug is not affected during the process of encapsulation and release with CS–PLA, CS–PLA–PEG and CS–PLA–PEG–G composite. In other experimental conditions, surfactant-free or PVA-stabilized RIF-loaded PLGA microspheres were shown to have no apparent effect

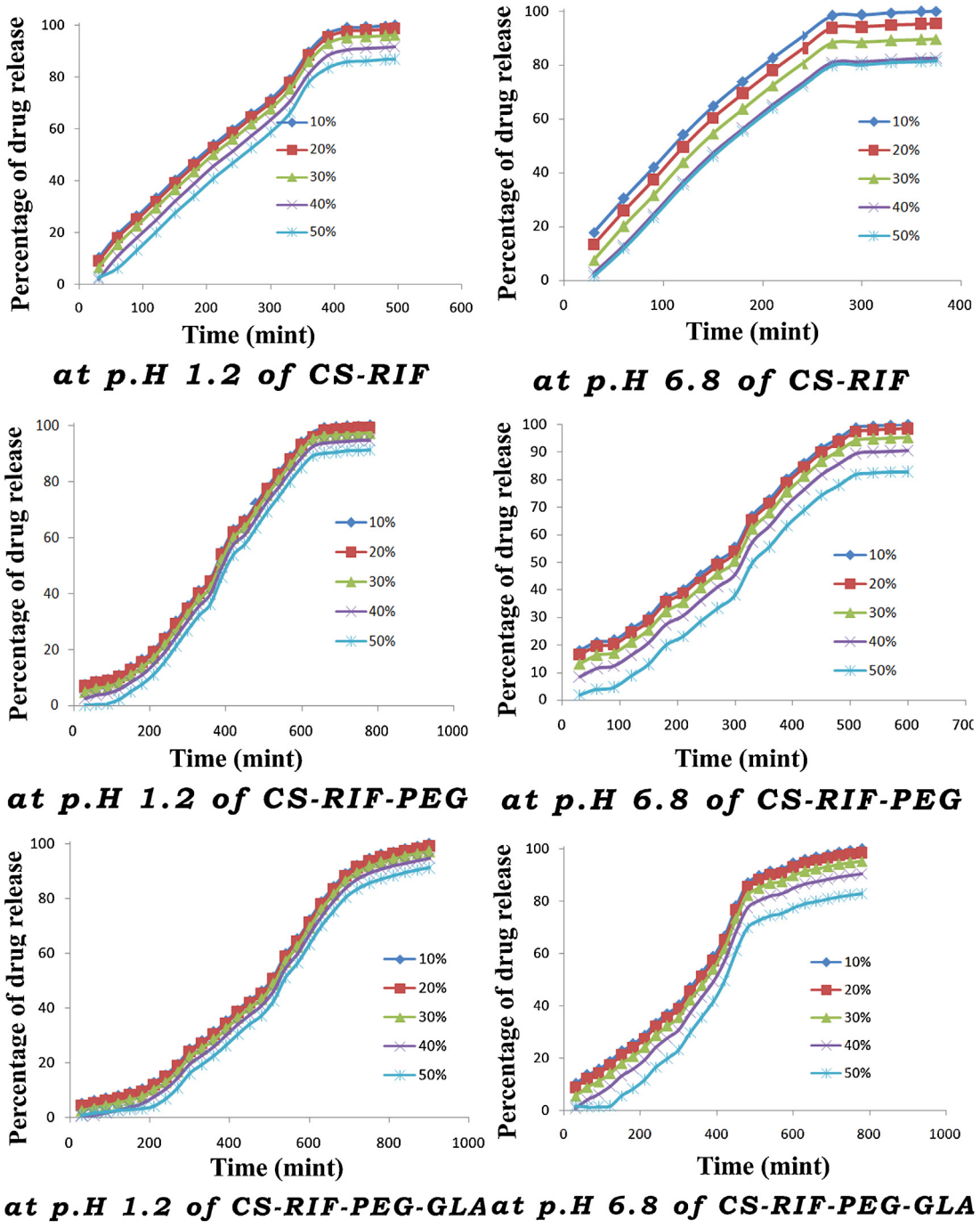

Fig. 5. In vitro analysis of rifampicin prepared nanoparticles.

Table 3
The relative cell viability of RIF, CS–PLA–RIF, CS–PLA–RIF–PEG and CS–PLA–RIF–PEG–G nanoparticles.

Nanoparticles	CTL		10 μg		20 μg		50 μg		100 μg	
RIF	101.0	94.0	40.0	44.0	30.1	27.3	16.48	14.0	10.0	4.0
CS–PLA–RIF, and	100.0	102.0	79.0	83.0	69.6	72.0	59.48	62.0	54.0	38.0
CS–PLA–RIF–PEG	105.0	103.0	81.0	83.0	71.5	70.0	61.48	59.0	52.0	59.0
CS–PLA–RIF–PEG–G	104.0	100.0	99.0	103.0	89.4	86.0	59.48	65.0	40.0	42.0

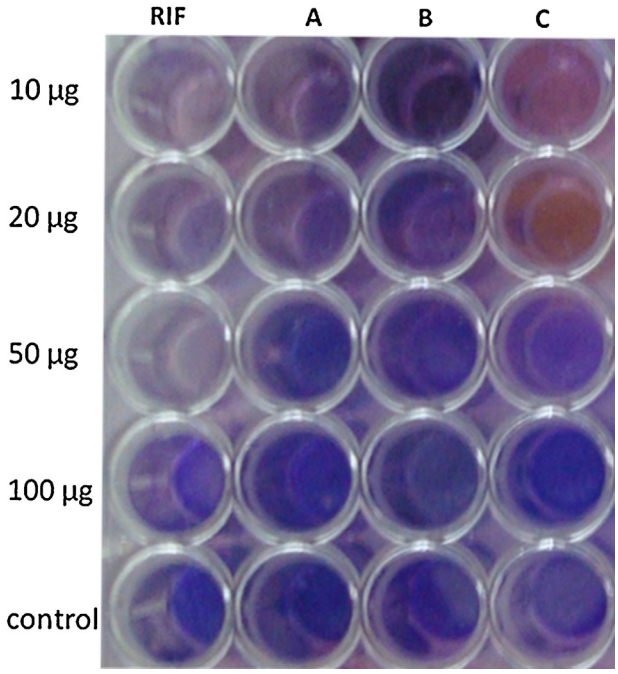

Fig. 6. The relative cell viability of free RIF and CS–PLA–RIF, CS–PLA–RIF–PEG, CS–PLA–RIF–PEG–G with various concentrations.

on viability of various macrophages cell lines over at least 4 h (Hirota et al., 2007, 2010). This is an important result from the point of application of such drug delivery systems.

4. Conclusion

The use of CS in combination with PEG and G shows the potential as new compression coats for controlled drug delivery. These coatings are able to suppress the release of RIF until it reaches the target place. The different pendant groups present in the composites have been ascertained by FTIR studies. From the SEM analysis, the homogeneity of the blends has been predicted. The drug release is based on time and pH controlled system due to the water insolubility of RIF and the matrix formation of CS–PLA/PEG/G, the solubility of which depends on the pH of the media. Drug permeation and in vitro test suggested for further study in the development of in vivo drug delivery system. Consequently, these systems show great promise with regard to the circumvention of the present limitations in the management of tuberculosis diseases. These results indicated that RIF coated CS–PLA/PEG/G nanoparticles could be a potential carrier for the controlled drug delivery. Furthermore the in vivo evaluation is in progress.

Acknowledgements

One of the authors M.Rajan is grateful to University grant commission (UGC), Government of India, for providing the fund under the scheme of "UGC-Dr. D.S. Kothari Post Doctoral fellowship" (Ref: No. F.4-2/2006 (BSR)/13-506-2011 (BSR)).

References

Ashish Dev, Binulal, N. S., Anitha, A., Nair, S. V., Furuike, T., Tamura, H., et al. (2010). Preparation of poly(lactic acid)/chitosan nanoparticles for anti-HIV drug delivery applications. *Carbohydrate Polymers*, *80*, 833–838.

Booysen, L. L., Kalombo, L., Brooks, E., Hansen, R., Gilliland, J., Gruppo, V., et al. (2013). In vivo/in vitro pharmacokinetic and pharmacodynamic study of spray-dried poly-(dl-lactic-co-glycolic) acid nanoparticles encapsulating rifampicin and isoniazid. *International Journal of Pharmaceutics*, *444*(2013), 10–17.

Centers for Disease Control. (2000). Targeted tuberculin testing and treatment of latent tuberculosis infection. *MMWR Recommendations and Reports*, *49*, 1–51.

Chan, J., Chan, H., Prestidge, C., Denman, J., Young, P., & Traini, D. (2013). A novel dry powder inhalable formulation incorporating three first-line anti-tubercular antibiotics. *European Journal of Pharmaceutics and Biopharmaceutics*, *83*, 285–292.

Changsan, N., Chan, H. K., Separovic, F., & Srichana, T. (2009). Physicochemical characterization and stability of rifampicin liposome dry powder formulations for inhalation. *Journal of Pharmaceutical Sciences*, *98*, 628–639.

Chen, H. L., Yang, W. Z., Chen, H., Liu, L. R., Gao, F. P., Yang, X. D., et al. (2009). Surface modification of mitoxantrone-loaded PLGA nanospheres with chitosan. *Colloids and Surface B: Biointerfaces*, *73*, 212–218.

Chen, M., Liu, Y., Yang, W., Li, X., Liu, L., Zhou, Z., et al. (2011). Preparation and characterization of self-assembled nanoparticles of 6-O-cholesterol-modified chitosan for drug delivery. *Carbohydrate Polymers*, *84*, 1244–1251.

Coban, A. Y., Birinci, A., Ekinci, B., & Durupinar, B. (2004). Drug susceptibility testing of *Mycobacterium tuberculosis* by the broth microdilution method with 7H9 broth. *Memorias do Instituto Oswaldo Cruz*, *99*, 111–113.

Desai, K. G. H., & Park, H. J. (2005). Preparation and characterization of drug-loaded chitosan–tripolyphosphate microspheres by spray drying. *Drug Development Research*, *64*, 114–128.

Du Toit, L. C., Pillay, V., & Danckwerts, M. P. (2006). Tuberculosis chemotherapy: Current drug delivery approaches. *Respiratory Research*, *19*(7), 118.

Geng, L., Yonglong, Z., Qing, M., Mozhen, W., & Yuee, F. (2008). Preparation characterization and aggregation behavior of amphiphilic chitosan derivative having poly (L-lactic acid) side chains. *Carbohydrate Polymer*, *72*, 60–66.

Gumbo, T., Louie, A., Deziel, M. R., Liu, W., Parsons, L. M., & Salfinger, M. (2007). Concentration dependent *Mycobacterium tuberculosis* killing and prevention of resistance by rifampin. *Antimicrobial Agents and Chemotherapy*, *51*, 3781.

He, D., Deng, P., Yang, L., Tan, Q., Liu, J., Yang, M., et al. (2013). Molecular encapsulation of rifampicin as an inclusion complex of hydroxypropyl-β-cyclodextrin: Design; characterization and in vitro dissolution. *Colloids and Surfaces B: Biointerfaces*, *103*, 580–585.

Hillmyer, M. A. (2007). Micelles made to order (A perspective). *Science*, *317*, 604.

Hirota, K., Hasegawa, T., Hinata, H., Ito, F., Inagawa, H., Kochi, C., et al. (2007). Optimum conditions for efficient phagocytosis of rifampicin loaded PLGA microspheres by alveolar macrophages. *Journal of Controlled Release*, *119*, 69–76.

Hirota, K., Hasegawa, T., Nakajima, T., Inagawa, H., Kohchi, C., Soma, G., et al. (2010). Delivery of rifampicin–PLGA microspheres into alveolar macrophages is promising for treatment of tuberculosis. *Journal of Controlled Release*, *142*, 339–346.

Huwyler, J., Wu, D., & Pardridge, W. M. (1996). Brain drug delivery of small molecules using immunoliposomes. *Proceedings of the National Academy of Sciences of the United States of America*, *93*, 14164–14169.

Jayakumar, R., Reis, R. L., & Mano, J. F. (2006). Phosphorous containing chitosan beads for controlled oral drug delivery. *Journal of Bioactive and Compatible Polymers*, *21*(4), 327–340.

Jelvehgari, M., Nokhodchi, A., Rezapour, M., & Valizadeh, H. (2010). Effect of formulation and processing variables on the characteristics of tolmetin microspheres prepared by double emulsion solvent diffusion method. *Indian Journal of Pharmaceutical Sciences*, *72*, 72–78.

Klaudt, K. (2000). The political causes and solutions of the current tuberculosis epidemic. In J. Whitman (Ed.), *The politics of emerging and resurgent infectious diseases*. London: MacMillan Press.

Kweon, D. K., & Kang, D. W. (1999). Drug-release behavior of chitosan-g-poly(vinyl alcohol) copolymer matrix. *Journal of Applied Polymer Science*, *74*, 458–464.

Langer, R. (2001). Perspectives: Drug delivery – Drugs on target. *Science*, *293*, 58.

Mehta, S. K., & Jindal, N. (2013). Formulation of tyloxapol niosomes for encapsulation stabilization and dissolution of anti-tubercular drugs. *Colloids and Surfaces B: Biointerfaces*, *101*, 434–441.

Mehta, S. K., Bhasin, K. K., Mehta, N., & Dham, S. (2005). Behavior of rifampicin in association with cylodextrin in aqueous media: A spectroscopic and conductometric study. *Colloid and Polymer Science*, *283*, 532.

Papadimitriou, S., Bikiaris, D., Avgoustakis, K., Karavas, E., & Georgarakis, M. (2008). Chitosan nanoparticles loaded with dorzolamide and pramipexole. *Carbohydrate Polymers*, *73*, 44–54.

Rahul, M. R., Amol, V. J., & Douglas, E. H. (2010). Poly(lactic acid) modifications. *Progress in Polymer Science*, *35*, 338.

Rajan, M., & Raj, V. (2012). Encapsulation characterisation and in-vitro release of anti-tuberculosis drug using chitosan–poly ethylene glycol nanoparticles. *International Journal of Pharmacy and Pharmaceutical Sciences*, *4*, 255–259.

Rashidova, S. Sh., Milusheva, R. Yu., Semenova, L. N., Mukhamedjanova, M. Yu., Voropaeva, N. L., Vasilyeva, S., et al. (2004). Characteristics of interactions in the pectin–chitosan system. *Chromatographia*, *59*, 779–782.

Schreiber, J., Zissel, G., Greinert, U., Schlaak, M., & Muller-Quernheim, J. (1999). Lymphocyte transformation test for the evaluation of adverse effects of anti-tuberculous drugs. *European Journal of Medical Research*, *4*, 67.

Singh, H., Bhandari, R., & Indu Pal, K. (2013). Encapsulation of rifampicin in a solid lipid nanoparticulate system to limit its degradation and interaction with isoniazid at acidic pH. *International Journal of Pharmaceutics*, *446*, 106–111.

Sullivan, S. M., & Huang, L. (1986). Enhanced delivery to target cells by heat-sensitive immunoliposomes. *Proceedings of the National Academy of Sciences of the United States of America*, *83*, 6117.

(2013). *International Union Against Tuberculosis and Lung Disease*. The Union.

Tzong-Ming, W., & Cheng-Yang, W. (2006). Crystallization and melting behavior of poly(ε-caprolactone) under physical confinement. *Polymer Degradation and Stability*, *91*, 2198.

Wu, J., Kong, T., Yeung, K. W. K., Shum, H. C., Cheung, K. M. C., Wang, L., et al. (2013). Fabrication and characterization of monodisperse PLGA–alginate core–shell microspheres with monodisperse size and homogeneous shells for controlled drug release. *Acta Biomaterialia*, http://dx.doi.org/10.1016/j.actbio.2013.03.022

Yan, S., Changsheng, L., Yuan, Y., Xinyi, T., Fan, Y., & Xiaoqian, S. (2009). Long-circulating polymeric nanoparticles bearing a combinatorial coating of PEG and water-soluble chitosan. *Biomaterials*, *30*(12), 2340–2348.

Yang, X. D., Zhang, Q. Q., Wang, Y. S., Chen, H., Zhang, H. Z., & Gao, F. P. (2008). Self-aggregated nanoparticles from methoxy poly(ethylene glycol)-modified chitosan: Synthesis; characterization; aggregation and methotrexate release in vitro. *Colloids and Surface B: Biointerfaces*, *61*, 125–131.

Zhang, H. Z., Gao, F. P., Liu, L. R., Li, X. M., Zhou, Z. M., & Yang, X. D. (2009). Pullulan acetate nanoparticles prepared by solvent diffusion method for epirubicin chemotherapy. *Colloids and Surface B: Biointerfaces*, *71*, 19–26.